Applied Catalysis B: Environmental 125 (2012) 271–281

Contents lists available at SciVerse ScienceDirect

Applied Catalysis B: Environmental

journal homepage: www.elsevier.com/locate/apcatb

Ethanol electrocatalysis on gold and conducting polymer nanocomposites: A study of the kinetic parameters

Rakesh K. Pandey*, V. Lakshminarayanan

Raman Research Institute, C.V. Raman Avenue, Bangalore 560080, India

ARTICLE INFO

Article history:
Received 17 February 2012
Received in revised form 1 May 2012
Accepted 3 June 2012
Available online 12 June 2012

Keywords:
In situ electropolymerization
Catalysis
Electrochemistry
Conducting polymers
Nanocomposite

ABSTRACT

The study attempts to compare the electrocatalytic effect of gold nanoparticles dispersed conjugated polymers using activation energy, Tafel slopes and reaction orders for the evaluation of their performance. A simple and rapid in situ chemical and electrochemical method was adopted for the synthesis of gold and different conducting polymers nanocomposites on electrode surfaces. The method involves the polymerization of the monomer to yield the polymer nanocomposite film with dispersed gold nanoparticles. Polyaniline, polypyrrole, polythiophene and poly(3,4-ethylenedioxythiophene) are the four polymers studied in this work. A systematic comparison among the nanocomposites reveals that although all the conducting polymers have good catalytic activity in alkaline medium however polyaniline dispersed with gold nanoparticles has the best catalytic properties among them as evidenced by its very low activation energy, low onset potential and reproducible currents.

1. Introduction

Gold nanocomposites with conjugated polymers are well known as electrocatalyst for the electro-oxidation of small organic molecules and therefore they find potential applications in fuel cells. However, there are very few reports in literature directed toward the study of the kinetic parameters of the electro-oxidation reactions using these materials. Such a study can be expected to advance our understanding of the reaction which may help in the development of improved electrocatalysts for the fuel cell applications. There are many reports on the use of these polymers as electrocatalyst in many different applications, primarily with noble metals e.g. Pt, Pd, Rh and Au [1–10]. The organization of metal nanoparticles in 2 and 3-dimensional materials is a crucial step for the development of nanoelectronic applications. Conducting polymers (CPs) with π-conjugated backbones offer a fascinating environment for metal nanoparticles with the advantage to achieve very high dispersion of metallic particles and a conducting network of conjugated polymers linking them. The high porosity and extended structure of CPs allow electrocatalytic materials to properly disperse in a 3-dimensional structure. This makes maximum number of catalytic centers available for the reacting species and thus significantly improves the electrocatalytic performance. There is a need of an in-depth analysis or the comparison of the electrocatalytic activity of different conducting polymers and metal combinations. The present work is an attempt to discuss and figuring out the merits and demerits of Au-conducting polymers (Au-CPs) combinations for ethanol electro-oxidation reaction in alkaline medium. The superior activity of gold at high pH has been recently studied by Rodriguez et al. [11a], wherein it was shown that in alkaline medium even carbon monoxide plays an important supportive role, which results in high catalytic performance. In addition the hydroxyl ions play a crucial role of oxygen source during the course of oxidation. We believe that no single parameter or property can account for the high catalytic activity of the Au nanocomposite film. In effect, a combination of several parameters, such as the accessibility of the Au nanoparticles within the film for the OH^- adsorption, the role of different CP in the effective removal of the products of the reaction, stability of the CP film in the electrolyte, adhesion of the CP film to the surface etc., all of which play major roles in the catalytic performance.

There are many literature reports available on the use of gold tetrachloride ($AuCl_4^-$) as an oxidizing agent for the aniline oxidation [9,10]. Wang et al. [10] have in their work prepared polyaniline nanofibers and gold nanoparticles simultaneously by using chloroaurate ($AuCl_4^-$) as the oxidant. In the present work we have adopted a simple electrochemical method to produce Au-conducting polymer nanocomposite film. The polymer and gold nanocomposites were formed in situ during the galvanostatic deposition process in the presence of their respective monomers in hydrochloric acid with Au wire as anode and another gold electrode as cathode. The electrochemical process consists of the in situ polymerization of monomer and subsequent formation of Au-CP nanocomposite film on cathode. While this method is similar to

* Corresponding author.
E-mail address: rakes_pandey1@yahoo.co.in (R.K. Pandey).

0926-3373/$ – see front matter © 2012 Elsevier B.V. All rights reserved.
http://dx.doi.org/10.1016/j.apcatb.2012.06.002

our recent works on palladium and conducting polymer nanocomposites, we discuss the relative performance evaluation of Au and different CPs nanocomposite in this paper based on kinetic parameters of the oxidation reaction [12a,b].

Electrochemical preparation of metal nanoparticles is also known in the literature. A sacrificial anode technique was used to produce Pd nanoparticles which were stabilized with the help of tetraalkylammonium cation in the solution [13,14]. Pd ions in the solution migrate toward the cathode and then the reduction takes place on cathode. An electrophoretic deposition of positively charged protonated polyaniline colloidal suspension in acetonitrile was studied by Li et al. [15].

In our work the Au-CP nanocomposite containing positively charged moieties in it [16], electrophoretically deposits on the gold substrate as a thin film. The method is of particular significance due to the fact that it is a single step electrochemical method, which avoids the extra steps of the preparation of CPs separately and subsequent mixing of polymer and gold. The prepared nanocomposite film can be directly used for further studying its properties such as electrocatalytic activity. A high rate of electro-oxidation of ethanol in alkaline media was observed for nanocomposite modified electrode. The studies present here are very useful in the understanding of the formation of interesting nanocomposite structures from gold which are the potential catalytic materials in direct ethanol fuel cells (DEFCs). Ethanol seems to be an interesting and safer alternative to highly toxic methanol because a well established supply chain for ethanol already exists in most of the countries. The surface of the nanocomposite film was thoroughly characterized using scanning electron microscopy (SEM), energy dispersive X-ray analysis (EDAX), atomic force microscopy (AFM) and Fourier transform infrared spectroscopy (FTIR).

2. Experimental

2.1. Chemicals

All the chemical reagents used in this study were analytical grade reagents. Aniline (Merck), pyrrole and thiophene (Spectrochem) 3,4-ethylenedioxythiophene (EDOT) (Aldrich), ethanol and sulfuric acid (Merck), hydrochloric acid (Nice chemicals) and sodium dodecyl sulfate (SDS) (S. D. fine chemicals) were used in our study. Millipore water having a resistivity of 18.2 MΩ cm was used to prepare the aqueous solutions.

2.2. Substrates, electrochemical set-up and instruments for surface characterization

We have carried out the electrochemical characterization studies by coating different Au-CP films on a gold disc working electrode, which was constructed by carefully sealing a 99.99% pure gold wire (Arora Mathey) of 0.5 mm diameter with soda lime glass. This electrode has a geometric area of 0.002 cm^2. Prior to each use the gold disc electrode was polished with emery paper, followed by mild polishing in aqueous slurries of progressively finer alumina of sizes ranging from 1.0 to 0.3 to 0.05 μm on a microcloth. After this, the electrode was put in an ultrasonic cleaner containing Millipore Milli-Q water to remove attached alumina particles. Then, it was cleaned in a "piranha" solution, which is a mixture of 30% H_2O_2 and concentrated H_2SO_4 in 1:3 ratio. (*Caution*! *Piranha solution is very reactive with organic compounds*, *storing in a closed container and exposure to direct contact should be avoided*). Finally the electrode was again washed with copious amount of Millipore Milli-Q water.

Au-CP films were also deposited on larger area gold substrate (deposited on glass by vacuum evaporation with chromium underlayer) for SEM and EDAX studies. For galvanostatic deposition of nanocomposite film, a 0.5 mm thick Au wire of 99.9% purity (Advent, UK) was used as an anode and a gold electrode as the cathode. A conventional three-electrode electrochemical cell was used for ethanol electro-oxidation studies. A platinum foil of large surface area was used as the counter electrode and a saturated calomel electrode (SCE) as the reference electrode. The cell was cleaned thoroughly before each experiment and kept in a hot air oven at 100 °C for at least 1 h before the start of the experiment.

Galvanostatic deposition was carried out using an EG&G potentiostat (model 263A) in chronopotentiometry mode and interfaced to a PC through a GPIB card (National Instruments). SEM and EDAX studies were carried out using FESEM (Zeiss). AFM studies were carried out using Pico plus (Molecular Imaging) AFM in ac (tapping) mode with an n-doped silicon tip. The FTIR spectra were obtained using an FTIR 8400 model (SHIMADZU). The images obtained were raw images, which were plane corrected using the scanning probe image processor (SPIP) software (Image Metrology, Denmark). For precise temperature control a temperature controller (JULABO-Model F25) was used.

2.3. Optimization of the synthetic procedure for Au-CP nanocomposites on gold substrate

The nanocomposite preparation method can be summarized as following.

For the galvanostatic deposition of the nanocomposite, 50 mM of monomer (aniline for PANI, pyrrole for PPY, thiophene for PTP, and 3,4-ethylenedioxythiophene for PEDOT) solutions were prepared in 5 ml 0.1 M HCl. Au wire of 5 mm length and 0.5 mm diameter working as anode and an evaporated gold film electrode of 0.15 cm^2 area working as cathode were used. An intense gas evolution was observed at both the electrodes due to water electrolysis during the process. (*Caution*! *the cell should have gas outlets near both the electrodes*!) The deposition was also carried out at currents, lower and higher than 50 mA and it was observed that at low currents the nanocomposite film was not thick enough to carry out electrocatalytic experiments. At higher currents the Au-CP nanocomposite was not adhering enough on the cathode surface during the gas evolution. However, we found that the deposition at a current of 50 mA provides very good electrocatalytic activity and better adhesion. Therefore we have optimized the current value to 50 mA based on shorter time of deposition, improved electrocatalytic response and robust surface film. Therefore, for all the characterization studies of the film, all the specimens were deposited at the current of 50 mA unless otherwise stated.

The synthetic approach for all the Au-CP nanocomposite films is given below.

2.3.1. Au-PANI nanocomposite

In the beginning of the galvanostatic dissolution the aniline solution turned to light blue color from the colorless solution which finally, at the end of experiment turned to reddish-pink. Simultaneously, a dark brown colored film is formed on the cathode surface.

2.3.2. Au-PPY nanocomposite

The pyrrole solution which was colorless in the beginning of galvanostatic dissolution turned to black color soon after the start of the experiment, indicating of the formation of polypyrrole in the solution. The electrode is coated with the film of dark black color, simultaneously during the experiment.

2.3.3. Au-PTP nanocomposite

The colorless thiophene solution turned to light yellow color which remained the same after the completion of the galvanostatic

dissolution experiment. Simultaneously a light brown coating is formed on the electrode surface.

2.3.4. Au-PEDOT nanocomposite

The 3,4-ethylenedioxythiophene solution turned to blue color, soon after the start of the galvanostatic dissolution experiment and finally turned to dark blue solution at the end of the experiment. Simultaneously a black coating is formed on the electrode surface.

3. Results and discussion

3.1. Characterization of Au-PANI nanocomposites with SEM, EDAX, AFM and FTIR spectroscopy

Fig. 1 shows the SEM images of the Au-CP nanocomposite films deposited on the gold substrate. Fig. 1a shows the SEM images of Au-PANI nanocomposite film, it shows the spherical disc like features of diameter around 100–400 nm. In addition there are smaller features present on the surface of diameter around 50–100 nm. At different locations on the modified substrate we observed similar kind of features. Fig. S2 is high resolution SEM image of the Au-PANI nanocomposite film, it shows that the disc like features observed in Fig. 1a are actually composed of very fine particles of 5–10 nm size which appear to be the gold nanoparticles embedded in the PANI matrix.

Fig. 1b shows the SEM images of the Au-PPY coated surface. The images show flat triangular and rectangular kind of features with sharp edges. These features are 20–100 nm in size and spread throughout the surface. In addition to these features a few cauliflower like structures are also present on the surface showing the fractal morphology of the Au-PPY nanocomposite in those regions. Fig. S3 shows the high resolution SEM image of the Au-PPY nanocomposite film showing the nanostructured features of dimension around 10–20 nm.

Fig. 1c is the SEM images of the Au-PTP nanocomposite coated surface. Unlike the other Au-CP nanocomposites the Au-PTP SEM image shows the presence of dendritic structure of the nanocomposite. These dendritic structures are more than a μm in length. From the high resolution SEM image (Fig. S4), which shows a single dendrite structure in much better resolution, we observe that the side branches of the dendritic structure have diameter around 10–20 nm.

Fig. 1d is the SEM image of the Au-PEDOT nanocomposite coated surface. The image shows the presence of cauliflower like nanostructures throughout the surface. These features resemble to the flower like structure with fractal growth. The size of these structures varies from 20 nm to 100 nm. The flower like structures can grow as large as 500 nm as seen from the figure. In high resolution Fig. S5, the flower like fractal growth is clearly visible and it shows that the flower like structures are composed of small 10–30 nm features.

The above SEM imaging analysis shows that the structure of the Au-CP nanocomposite coated surface varies in the presence of different conducting polymers. This is an important observation as we can form varieties of nanostructures for various applications by this simple one step preparation method.

We have also carried out EDAX studies on all Au-CPs coated surfaces. Tables S1–S4 in supporting information show the EDAX elemental analysis results for Au-PANI, Au-PPY, Au-PTP and Au-PEDOT nanocomposite films, respectively. EDAX results show the presence of metallic Au and carbon in all the Au-CP nanocomposite films along with nitrogen (Au-PANI and Au-PPY) and sulfur (in Au-PTP and Au-PEDOT). The Au-PEDOT nanocomposite film also shows the presence of O and Na (from SDS). The EDAX analysis confirms the presence of Au and respective conducting polymers in all Au-CP nanocomposite films.

The 3-dimensional nature and the roughness parameters of the Au-CP nanocomposite films were studied using an AFM, operating in tapping mode. Fig. 2a–d shows the 5 μm × 5 μm AFM topographic images of Au-PANI, Au-PPY, Au-PTP and Au-PEDOT nanocomposite films, respectively. Au-PANI and Au-PTP nanocomposite films were found to be very rough while the roughness of Au-PPY and Au-PEDOT nanocomposite films was considerably less.

The roughness parameters, i.e. the average and rms roughness calculated from the respective 5 μm × 5 μm AFM images are presented in supporting information as Table S5. Au-PTP surface shows maximum roughness followed by Au-PANI, Au-PEDOT and Au-PPY surface.

Infra-red spectroscopy was performed on the coated material to check the chemical composition of the material. Fig. 3 shows the FTIR spectrum of the coated material in all the Au-CP nanocomposite films. Fig. 3a shows FTIR spectra of Au-PANI nanocomposite, the distinctive infra-red peaks for the conjugated polymer PANI are clear in the spectra. The peak at 1266 cm^{-1} is for the C—N stretch which is the usually observed characteristic infrared peak for the aromatic amines. In addition PANI infra-red spectra also show the characteristic peaks of benzenoid and quinoid form of the aromatic phenyl ring system. The two peaks at 1513 cm^{-1} and 1637 cm^{-1} are for the benzenoid and quinoid forms of the PANI, respectively. The presence of the above mentioned infrared peaks confirms the presence of the polymer form of aniline in the coated material [12a,17–21].

The integrated intensity of IR peaks at 1637 cm^{-1} (quinoid peak) and 1513 cm^{-1} (benzenoid peak) can be used to calculate the so called *R* value, which is the ratio of the area under the IR peaks at 1637 cm^{-1} and 1513 cm^{-1} [12a,17]. In Au-PANI nanocomposite the *R* value was calculated to be 0.91. This shows that there are more benzenoid rings than quinoid rings in the PANI. With the help of *R* value which is often related with the oxidation state of the PANI, we have defined the following structure of PANI in the coated material.

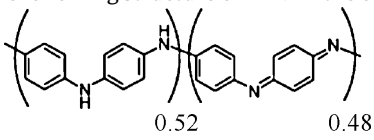

Fig. 3b shows the FTIR spectra of Au-PPY scraped out from the coated surface. The peaks at 1460 and 1377 cm^{-1} may be assigned to typical polypyrrole ring vibrations. The peaks at 721, 770 and 1160 cm^{-1} is assigned due to the =C—H out of plane vibrations and C—N stretching vibrations, respectively [22,23].

Fig. 3c shows the FTIR spectra of the Au-PTP scraped out from the coated surface. It shows a C=C aromatic ring stretch at 1555, 1460 and 1374 cm^{-1} and in-plane C—H deformation at 1027 and 1072 cm^{-1}. The spectra also show the C—S bending band at 850 cm^{-1} [22,24,25]. Fig. 3d is the FTIR spectra of the Au-PEDOT nanocomposite. The spectra show the infrared peaks at 1370, 1460, 1520 cm^{-1} for stretching mode of C—C and C=C in the thiophene ring. The peaks at 770 and 720 cm^{-1} are associated with the C—S bending vibration. The peaks at 1650, 1700 and 1750 cm^{-1} may be assigned to the doped state of the polymer [26]. In all the above mentioned cases the slight shift in the peak positions is due to the presence of gold atoms which are attached to the polymer and cause the change in the electron density.

3.2. Electrocatalytic activity of Au-CP nanocomposite film for ethanol oxidation

The electrocatalytic oxidation of small alcohols has been studied as the anodic reaction in direct alcohol fuel cells (DAFCs). The direct ethanol fuel cell is important for portable and remote power

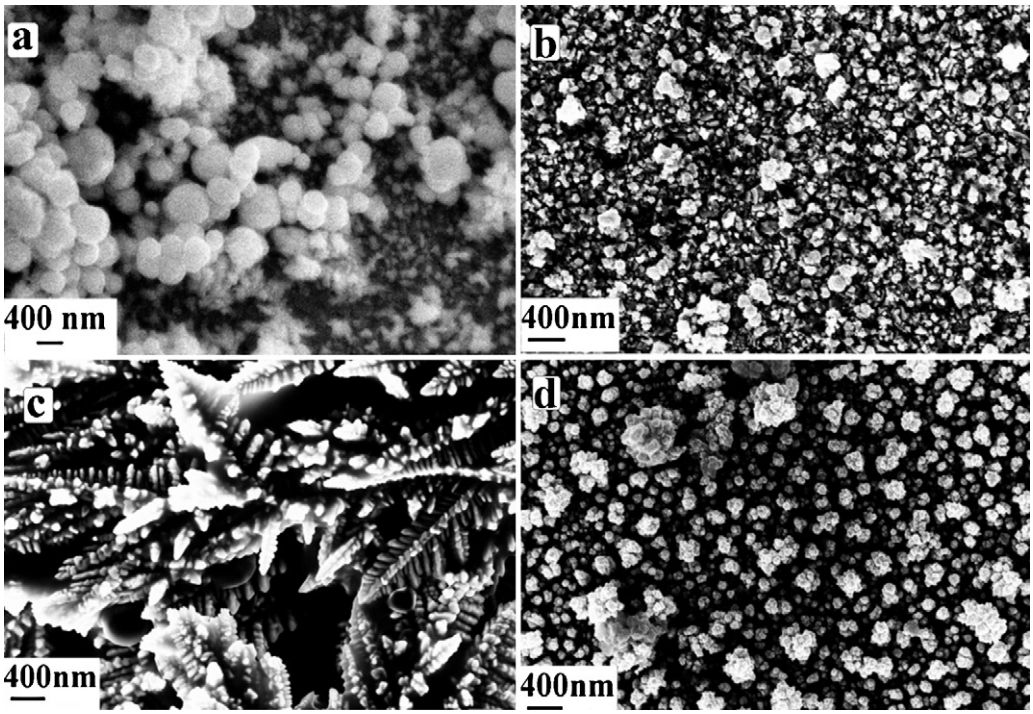

Fig. 1. (a) FESEM image of Au-PANI nanocomposite film (scale bar = 400 nm), (b) FESEM image of Au-PPY nanocomposite film scale bar = 400 nm, (c) FESEM image of Au-PTP nanocomposite film showing the dendritic growth of the nanostructures (scale bar = 400 nm) and (d) FESEM image of Au-PEDOT nanocomposite film shows the cauliflowers like fractal growth of the nanostructures (scale bar = 400 nm).

applications. Moreover the higher energy density (8.01 KWh kg^{-1}), lower toxicity and easy production through the fermentation of sugar make ethanol a better and safer alternative than other small organic molecules such as methanol, in direct fuel cells. The conducting polymer nanocomposites with gold are excellent catalytic material due to the high porosity, conducting nature and easy access of reacting species to the electrocatalytic centers.

We have evaluated the electrocatalytic activity of different Au-CP nanocomposite coated electrodes by studying ethanol electro-oxidation as a model system in alkaline medium of 0.5 M NaOH. In order to make sure the catalytic activity is due to the nanocomposite film, we have carried out experiment with bare gold substrate. In the case of bare gold we did not observe any significant catalytic activity toward ethanol electro-oxidation as seen in Fig. S1 of supporting information.

Fig. 4a–d shows the ethanol electro-oxidation voltammogram for the different Au-CP modified electrodes (a-Au-PANI, b-Au-PPY, c-Au-PTP and d-Au-PEDOT) in 1 M ethanol in 0.5 M NaOH. In all the cases we have carried out 200 potential cycles experiment in order to determine the reproducibility and stability of the

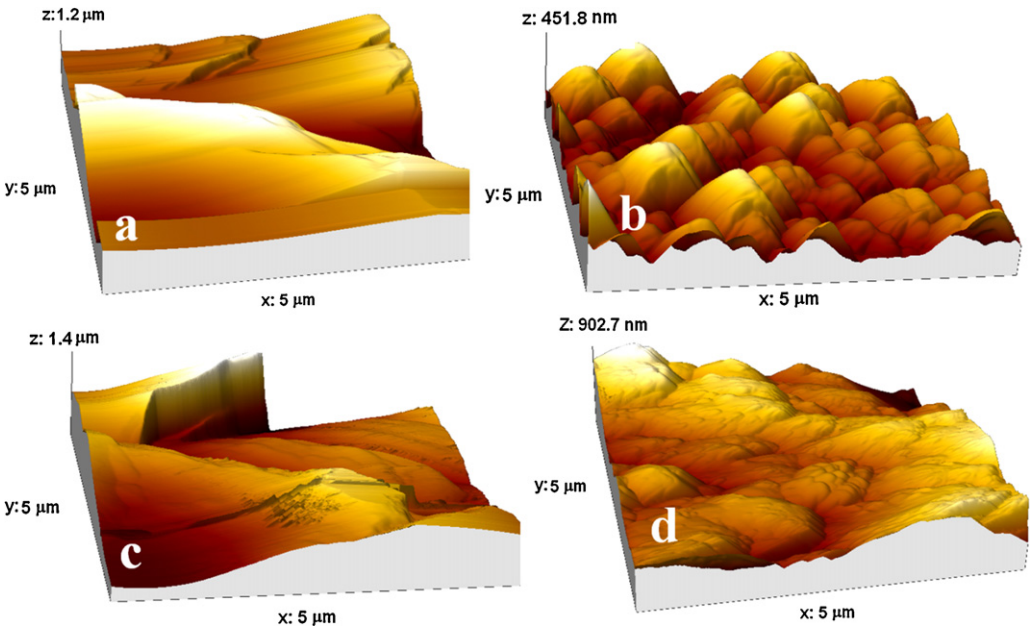

Fig. 2. AFM image of Au-CP nanocomposites (a) Au-PANI nanocomposite, (b) Au-PPY nanocomposite, (c) Au-PTP nanocomposite and (d) Au-PEDOT nanocomposite.

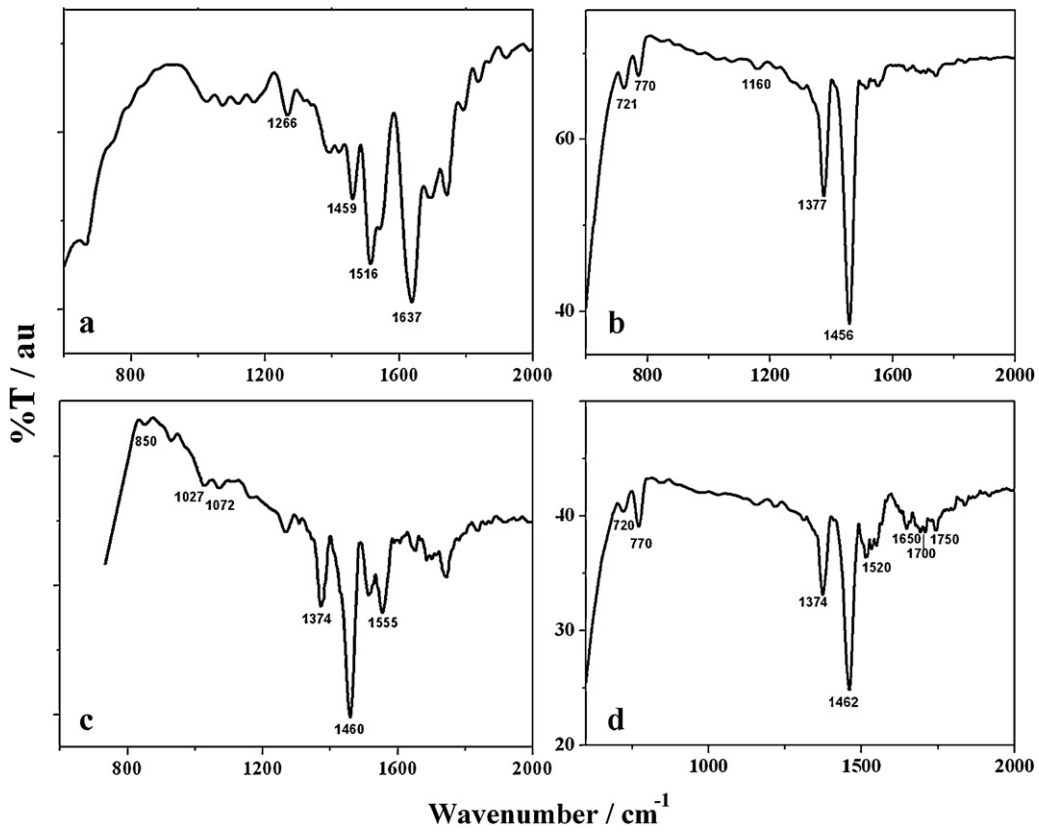

Fig. 3. FTIR spectra of Au-CP nanocomposites (a) Au-PANI nanocomposite showing the characteristic benzenoid and quinoid peaks for the PANI in the composite, (b) Au-PPY nanocomposite, (c) Au-PTP nanocomposite and (d) Au-PEDOT nanocomposite.

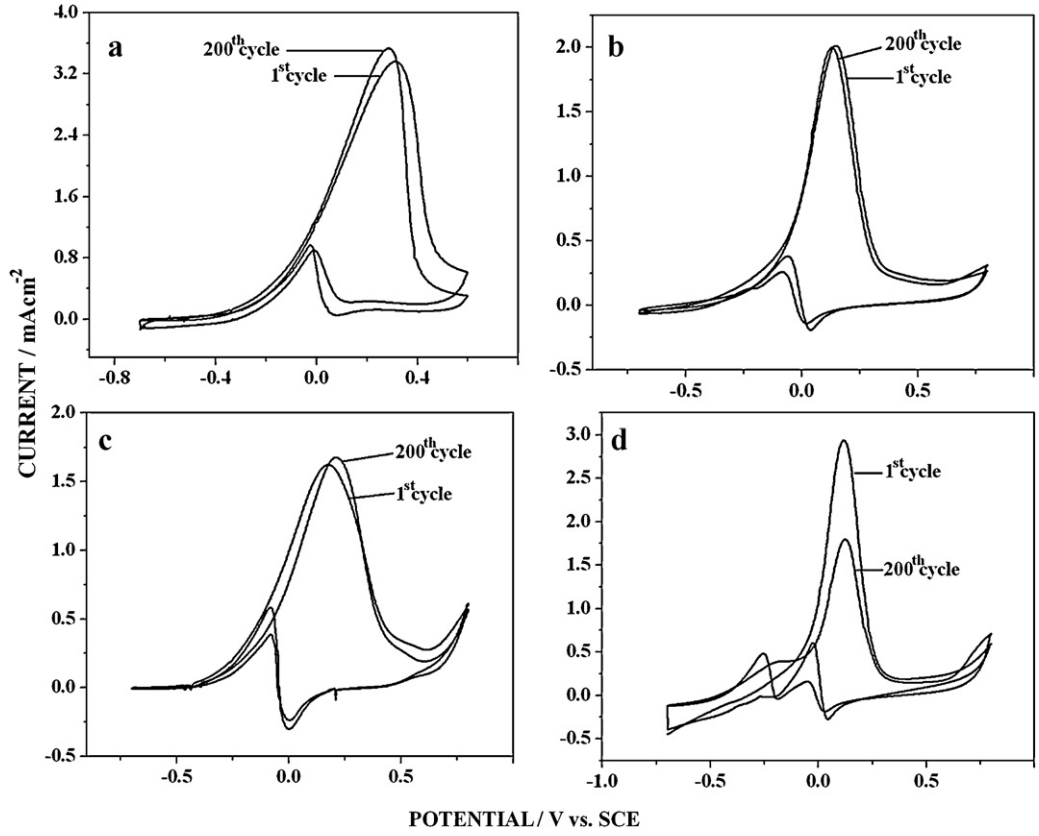

Fig. 4. (a) 200 cycles voltammogram for the electro-oxidation of 1.0 M ethanol in 0.5 M NaOH at different Au-CP nanocomposite film (a) Au-PANI nanocomposite film, (b) Au-PPY nanocomposite film, (c) Au-PTP nanocomposite film and (d) Au-PEDOT nanocomposite film.

Table 1
The ethanol electrocatalysis results obtained for different Au-CP nanocomposites in terms of onset potential, peak potential and peak current.

Nanocomposite	Onset potential (V)		Peak potential (V)		Peak current (mA cm^{-2})	
	1st cycle	200th cycle	1st cycle	200th cycle	1st cycle	200th cycle
Au-PANI	−0.34	−0.34	0.31	0.28	3.36	3.50
Au-PPY	−0.35	−0.40	0.14	0.12	2.02	2.00
Au-PTP	−0.40	−0.40	0.17	0.20	1.63	1.60
Au-PEDOT	−0.36	−0.36	0.11	0.12	2.93	1.80

nanocomposite modified electrode. All the current values are corrected to the respective effective catalytic surface area (ECSA), which represents the electrochemically accessible active sites on the electrode surface. ECSA of all Au-CP nanocomposite films was measured from the gold oxide stripping analysis carried out in 0.5 M sulfuric acid solution [27].

Table 1 shows the cyclic voltammetry results obtained for different Au-CP nanocomposites in terms of onset potential, peak potential and peak current. Among the four systems we have studied the Au-PTP system was found to be the best in terms of its onset potential for ethanol oxidation reaction. The Au-PTP modified electrode shows the lowest onset potential of −0.40 V followed by Au-PEDOT (−0.36 V), Au-PPY (−0.35 V) and Au-PANI (−0.34 V) modified electrodes. The onset potential was constant in all the four systems even after the 200 potential cycles. All the cyclic voltammetry experiments shown in the table were carried out at 100 mV s^{-1} scan rate and at room temperature.

The Au-PANI nanocomposite modified electrode was found to be the best in terms of peak current. The peak current of 3.36 mA cm^{-2} for the Au-PANI electrode was found to be the maximum among the four systems studied, which was closely followed by Au-PEDOT (2.93 mA cm^{-2}), Au-PPY (2.02 mA cm^{-2}) and Au-PTP (1.68 mA cm^{-2}). The peak current increased after 200 potential cycles in Au-PANI system to 3.53 mA cm^{-2}. The peak currents of Au-PPY and Au-PTP modified electrodes were unchanged after 200 potential cycles. The decline in the peak current was observed in Au-PEDOT modified electrode from 2.93 mA cm^{-2} to 1.80 mA cm^{-2}. This could be due to the instability of the Pd-PEDOT nanocomposite film.

Except for Au-PEDOT system which shows a 38% decline in the catalytic current, 200 cycles, CV experiment in Au-CP nanocomposite films shows no decline in the electro-oxidation current of ethanol. This shows that there is negligible poisoning of the catalytic surface due to any of the reaction products of ethanol oxidation. This is an important advantage of Au-CP nanocomposite electrodes as the electrode poisoning is a major problem in electro-oxidation reactions of alcohols.

During the reverse scan there is a secondary peak in all the Au-CP nanocomposite systems. This reverse anodic peak behavior can be explained as due to the fact that the Au atoms are not in equilibrium with the metallic lattice after the reduction of blocking oxide film and therefore the high energy sites possess excellent catalytic activity [28a,b].

The well known and established reaction mechanism for the electro-oxidation of ethanol in alkaline medium involves the oxidation of ethanol to acetate ions at the anode. The different steps of the reaction can be summarized as following [29–32].

$$C_2H_5OH + 3OH^- \rightarrow CH_3CO_{ads} + 3H_2O + 3e^- \quad (1)$$

$$OH^- \rightarrow OH_{ads} + 1e^- \quad (2)$$

$$CH_3CO_{ads} + OH_{ads} \rightarrow CH_3COOH \quad (3)$$

$$CH_3COOH + OH^- \rightarrow CH_3COO^- + H_2O \quad (4)$$

In all the nanocomposite systems the onset potential is more negative and the current is more than the previous reported values for ethanol electro-oxidation on porous gold nanoparticles film [31,32]. This shows that the combination of conducting polymer and gold in the form of nanocomposite serves as a better electrocatalyst for ethanol oxidation than gold nanoparticles alone.

3.3. Kinetics of ethanol electro-oxidation

3.3.1. Activation energy (E_a) determination and Tafel plot analysis for ethanol electro-oxidation

Fig. 5 shows the cyclic voltammograms for ethanol oxidation at different temperatures for all Au-CP nanocomposite films. In all the Au-CP nanocomposite films it is clear from the figure that the ethanol electrocatalysis currents have increased with the temperature and also the onset potentials have become more negative. The change in the onset potential at higher temperature indicates the low activation energy requirement at higher temperatures. This is due to the higher catalytic activity of the nanocomposite at elevated temperatures. In addition the presence of OH_{ads} is in fact helpful in achieving high electro-oxidation current. Adsorbed hydroxyl groups also play crucial role in suppressing the formation of poisoning species [33–36]. The adsorption of hydroxyl ions on gold has been a well established fact in the literature [11,37–39]. The adsorption plays a key role in determining the catalytic properties of gold electrode for electro-oxidation of small organic molecules and any process which accelerates or enhances the adsorption of hydroxyl ions would eventually improve the catalytic activity. The low onset potential values at high temperatures probably indicate the enhanced adsorption of hydroxyl ions [11,40]. At high temperatures we observed an increase in the anodic current of reverse potential scan. This current eventually becomes higher than the anodic current of the forward potential scan. The increase in the reverse current is the consequence of the enhanced catalytic reaction during the initial potential scan and this indicates that there are more active centers or high energy sites available for the reaction.

The plot between log I and $1/T$ also called as the Arrhenius plots, for ethanol oxidation on all Au-CP electrodes at different potentials, near the foot of the cyclic voltammogram (−500 mV to −100 mV) are shown in Fig. 6. A very good linear relationship can be seen from these plots. This shows that the mechanism of ethanol electro-oxidation remains the same at all the temperatures. The apparent activation energies were calculated from the slope of those curves (slope = $-E_a/2.3R$), R being the gas constant. The activation energy values are labeled adjacent to their respective plots. The average E_a values for different Au-CP films in the potential range studied are 37.0 KJ mole^{-1}, 56.7 KJ mole^{-1}, 57.0 KJ mole^{-1} and 56.7 KJ mole^{-1} for Au-PANI, Au-PPY, Au-PTP and Au-PEDOT nanocomposite films. It is clear that the E_a required for the Au-PANI system is the lowest among all the Au-CP systems, this is followed by Au-PTP system. Au-PPY and Au-PEDOT have almost same values activation energy required. The lower E_a value in the case of Au-PANI system than other Au-CP systems can be accounted due to the small size particles, associated with higher catalytic activity being present on the surface as seen in the SEM image. The values obtained of E_a are comparable to the values observed for Pt, Pd and Au based catalytic materials [41–43].

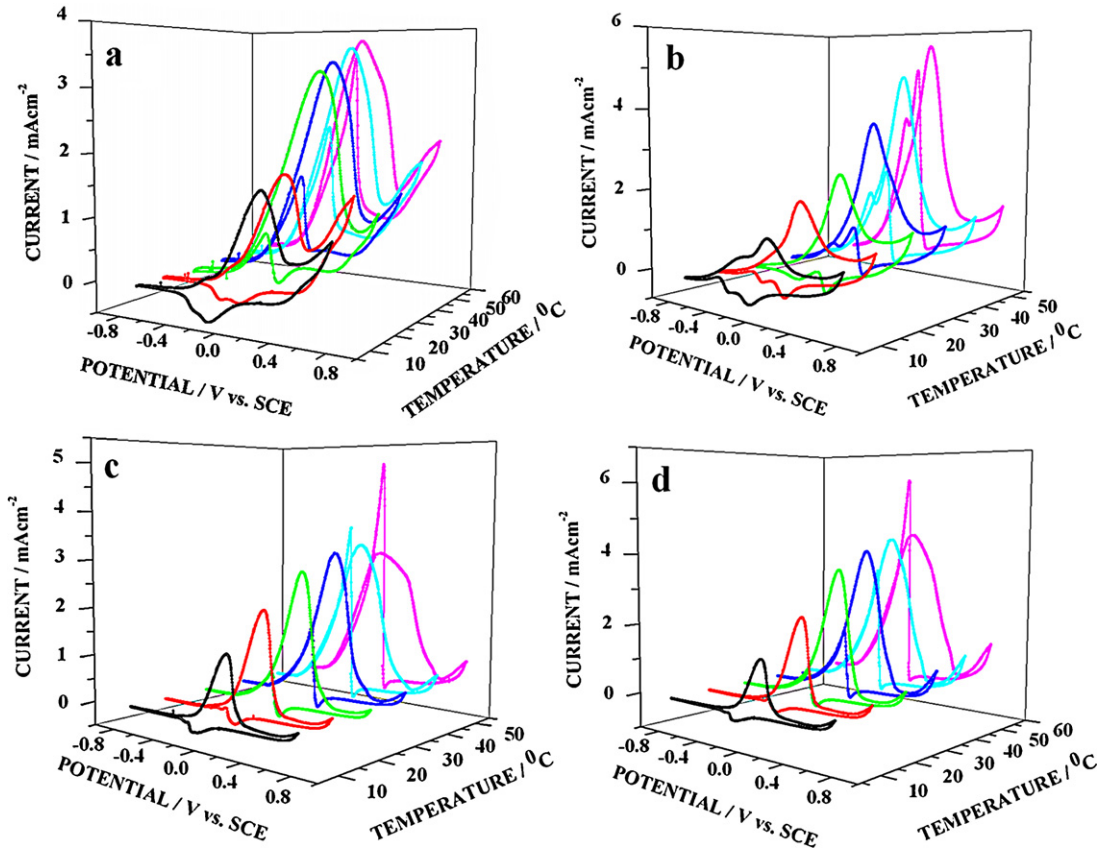

Fig. 5. (a) Cycle voltammograms for the electro-oxidation of 1.0 M ethanol in 0.5 M NaOH at different Au-CP nanocomposite film at different temperatures (a) Au-PANI nanocomposite film, (b) Au-PPY nanocomposite film, (c) Au-PTP nanocomposite film and (d) Au-PEDOT nanocomposite film.

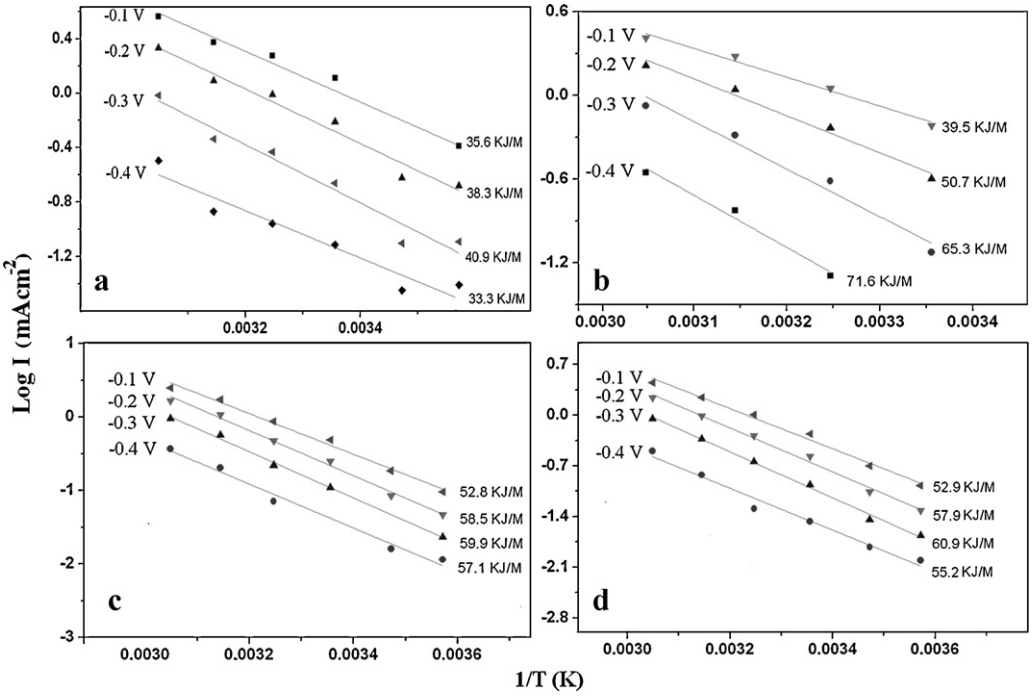

Fig. 6. (a) log *I* vs. 1/*T* (Arrhenius plots) for different Au-CP nanocomposite film at different potentials, corresponding activation energy values are labeled adjacent to the curves. (a) Au-PANI nanocomposite film, (b) Au-PPY nanocomposite film, (c) Au-PTP nanocomposite film and (d) Au-PEDOT nanocomposite film.

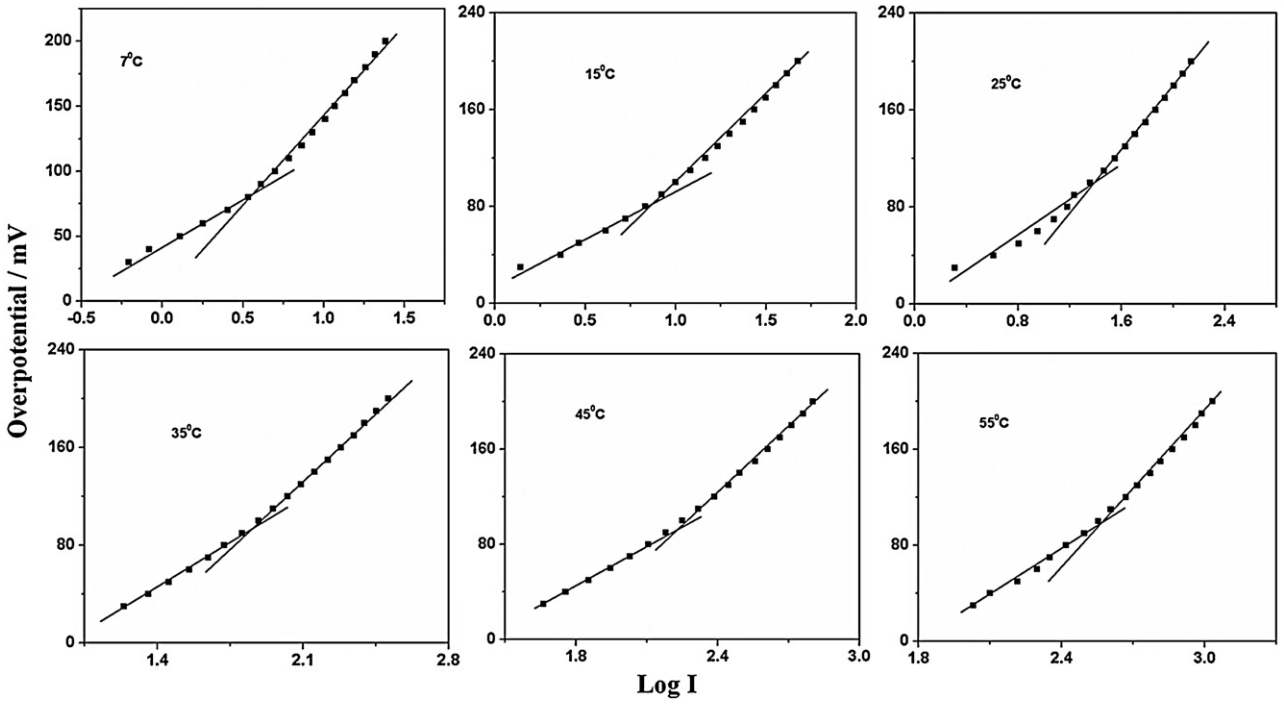

Fig. 7. Tafel plots (overpotential (η vs. $\log I$ (mA cm^{-2})) for Au-PANI nanocomposite at different temperatures and the fitting for two slopes.

It can be seen that the Tafel slopes are unusually large for all systems except Au-PANI electrode. This shows that the extent of contamination and surface blocking by adsorbed intermediates are minimum in the case Au-PANI compared to other polymers. Figs. 7–10 show the Tafel plots for the different Au-CP systems Au-PANI (Fig. 7), Au-PPY (Fig. 8), Au-PTP (Fig. 9) and Au-PEDOT (Fig. 10). The values of the slopes for all the Au-CP systems are given in Table 2.

The plots of Au-PANI and Au-PTP systems fit for the two slopes at lower and higher overpotentials, with the first slope value lower than the second slope as can be seen from Figs. 7 and 9. The values of both the first and second slopes increase steadily with the temperature. The higher slope values at higher temperatures indicate the enhanced adsorption of intermediate carbonaceous species, formed after the ethanol electro-oxidation reaction, on the electrode surface at elevated temperatures. These adsorbed species

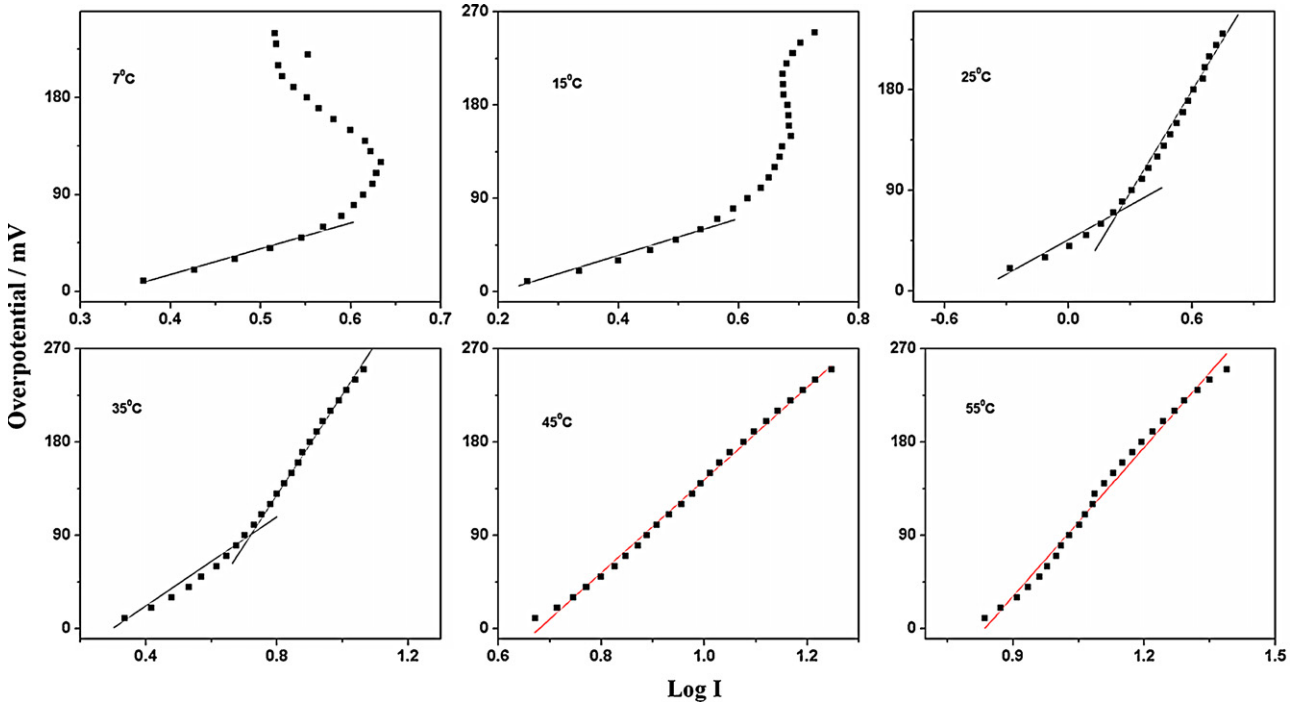

Fig. 8. Tafel plots (overpotential (η vs. $\log I$ (mA cm^{-2})) for Au-PPY nanocomposite at different temperatures and the fitting for first slope at 7 °C, 15 °C two slopes at 25 °C and 35 °C and linear curve at 45 °C and 55 °C.

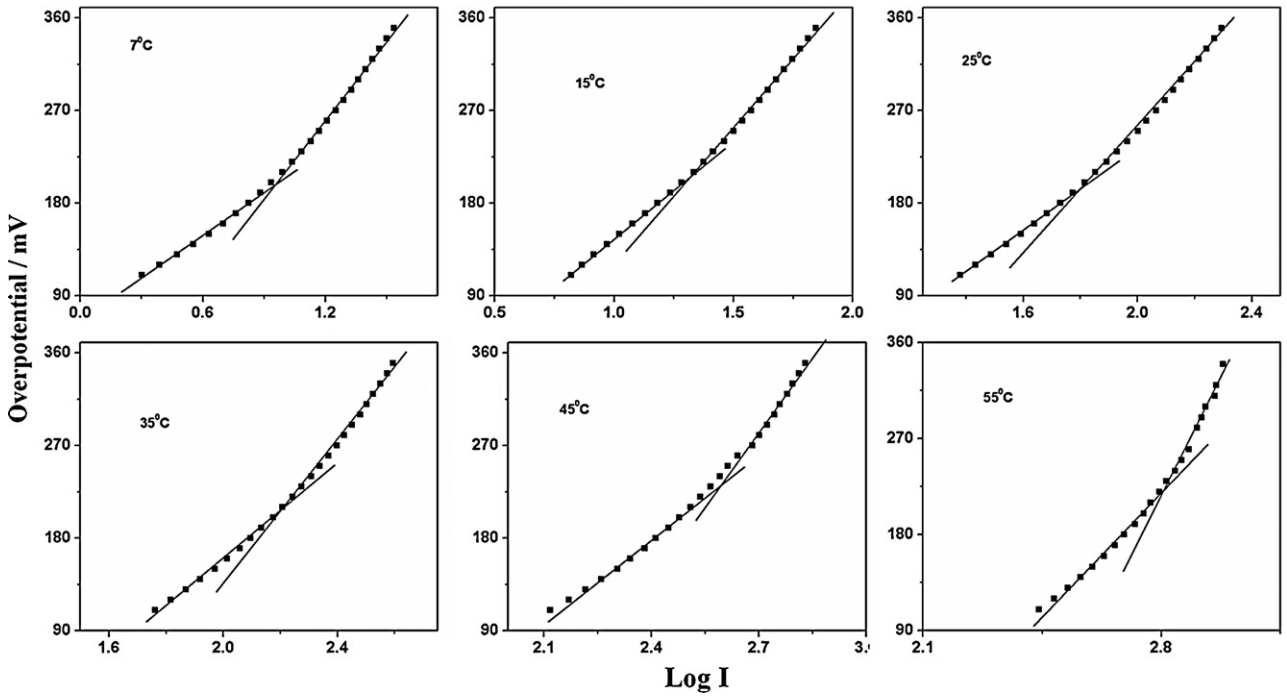

Fig. 9. Tafel plots (overpotential (η vs. $\log I$ (mA cm^{-2})) for Au-PTP nanocomposite at different temperatures and the fitting for two slopes.

may block the available active sites and can only be oxidized at very high overpotentials. The values of the first slope (at lower overpotentials) can be compared to those of the second slopes (at higher overpotentials). It can be seen that second slope values are always higher than the first slope. Since the electrocatalysis currents are not mass transfer controlled as known from the literature, this indicates that as the reaction progresses impurities weakly get adsorbed on the surface, which can only be removed at very high anodic overpotentials [43–45]. The higher slope values of both the slopes (first and second) in Au-PTP system than that of Au-PANI system indicate that the reaction is more favored in the case of Au-PANI system than Au-PTP system.

Tafel plot analysis of Au-PPY system (Fig. 8) shows completely different behavior with temperature. At lower temperatures (7 and 15 °C) the Tafel plot which is linear in the beginning (lower overpotentials) tends to become nonlinear at higher overpotentials. Plots fit well for two slopes at intermediate temperatures (25 and 35 °C) and at elevated temperatures (45 and 55 °C) the plots fit for a linear

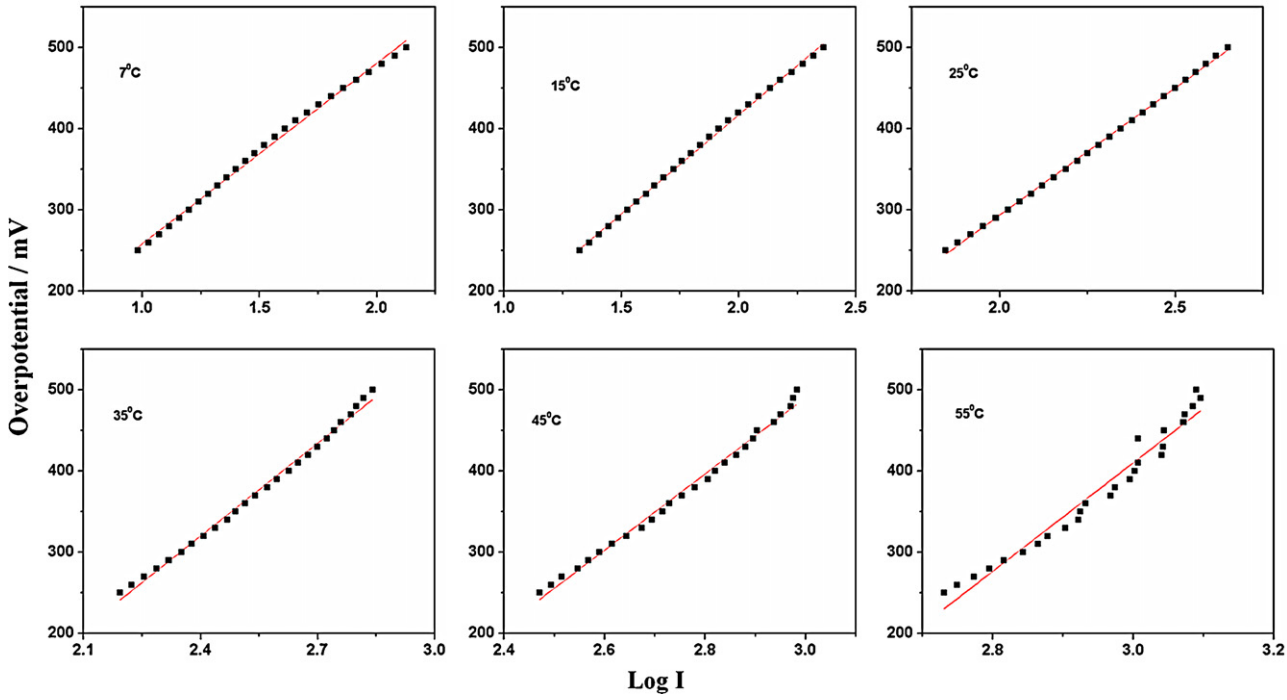

Fig. 10. Tafel plots (overpotential (η vs. $\log I$ (mA cm^{-2})) for Au-PEDOT nanocomposite at different temperatures and the fitting for a linear curve.

Table 2
The Tafel slopes for ethanol electrocatalysis obtained at different temperatures for different Au-CP nanocomposites.

Temperature (°C)	Slopes							
	Au-PANI		Au-PPY		Au-PTP		Au-PEDOT	
	1st	2nd	1st	2nd	1st	2nd	1st	2nd
7	65.8	144.7	247.0	–	137.2	248.0	222.0	–
15	73.6	146.2	173.0	–	191.2	269.7	243.0	–
25	63.1	129.0	98.6	308.0	202.9	308.0	313.0	–
35	106.3	160.1	192.0	449.0	223.0	360.0	381.0	–
45	118.1	184.8	447.0	–	269.0	445.0	469.0	–
55	132.0	211.8	479.0	–	319.3	650.0	668.0	–

curve. Unlike Au-PANI and Au-PTP systems the Tafel plots of Au-PEDOT system can be fitted for one slope at all the temperatures as can be seen from Fig. 10. Au-PEDOT system also shows the trend of higher slope values with increasing temperature. The slope values are much higher than those of Au-PANI system. The presence of a linear curve throughout the potential range and higher slopes values perhaps indicate that the effect of adsorption of impurities does not vary too much as the reaction progress.

The term Tafel slope does not have its usual significance in ethanol oxidation as it has in defining the fundamental processes in electrode kinetics. The term is used only to indicate the slope of the semilogarithmic plot of current vs. voltage. This is due to the fact that the straight line between overpotential and log I is not generally obtained in the case of alcohol oxidation reaction [45]. In this case, the interpretation of the Tafel slopes is not very straightforward due to the adsorption of the reaction intermediates. This results in surface poisoning, which leads to the observation of nonlinearity in the plot. Nevertheless, the Tafel slope can be a reliable indicator for the understanding of reaction mechanism and its temperature dependence. Au-PANI system shows the lowest slope values among all the Au-CP systems studied in this work. This suggests us that the Au-PANI is the best catalytic material for the ethanol electro-oxidation reaction. This also confirms the low activation energy values required for ethanol electro-oxidation in Au-PANI system.

The reaction order with respect to ethanol was also calculated by plotting the log I vs. log c (ethanol concentration) for all Au-CP nanocomposite films as shown in Fig. 11. The order was calculated by using the following equations: [41]

$$I = nFkc^m \text{ and } \log I = \log nFk + m \log c$$

where F is the Faraday's constant, k is the reaction constant, c is the ethanol concentration and m is the reaction order with respect to ethanol.

The slope of the log I vs. log c plot, at any constant temperature can be used to calculate the apparent reaction order (m) of ethanol electro-oxidation reaction with respect to the ethanol concentration [41,44,45]. We have calculated the order at two different potentials −0.2 V and 0.0 V. The values of reaction order are shown in Table 3. There is a change in the reaction order at different potentials in all the Au-CP systems except the Au-PANI system. Reaction order of Au-PANI remains the same at both the potentials with a

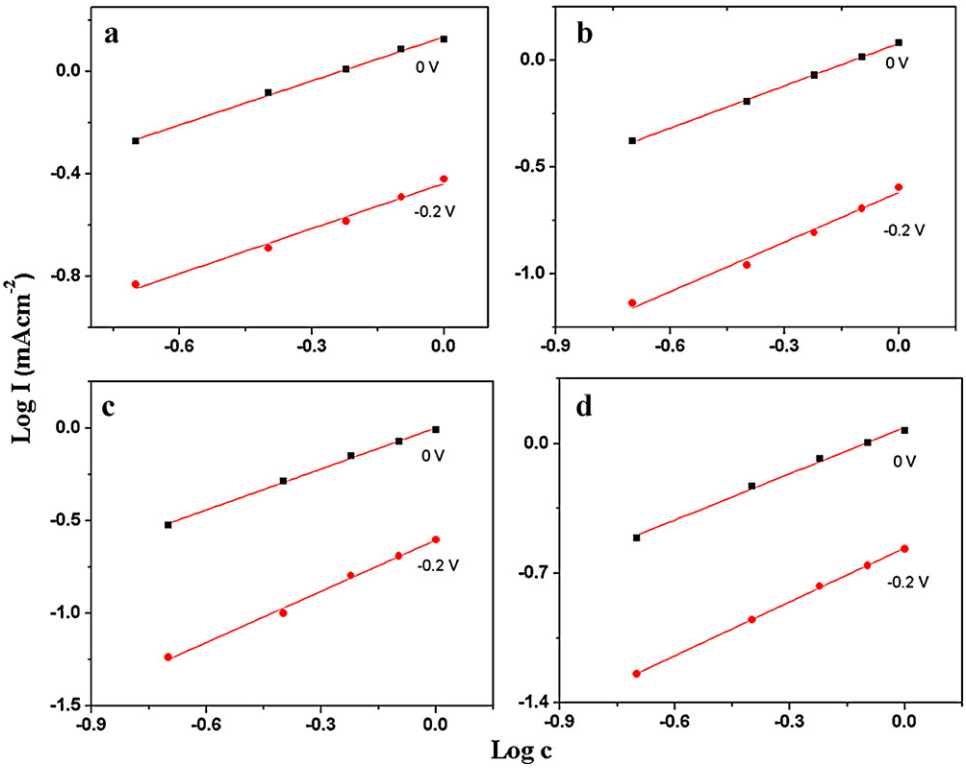

Fig. 11. (a) log I vs. log c plots for different Au-CP nanocomposite film at two different potentials (a) Au-PANI nanocomposite film, (b) Au-PPY nanocomposite film, (c) Au-PTP nanocomposite film and (d) Au-PEDOT nanocomposite film.

Table 3
The calculated reaction order with respect to ethanol concentration for different Au-CP nanocomposites.

Nanocomposite	Reaction order	
	−0.2 V	0.0 V
Au-PANI	0.57	0.57
Au-PPY	0.77	0.66
Au-PTP	0.92	0.74
Au-PEDOT	0.97	0.83

value of 0.57. This shows that the reaction mechanism for ethanol oxidation is fundamentally same at different potentials. The slight change in the reaction order in Au-PPY, Au-PTP and Au-PEDOT systems can be seen from Table 3, the reaction order is more at lower overpotentials (−0.2 V) and less at higher overpotentials (0 V) for all the nanocomposite films except Au-PANI.

4. Conclusions

In conclusion a novel one step electrochemical method to prepare gold and different conducting polymers namely polyaniline, polypyrrole, polythiophene and poly(3,4-ethylenedioxythiophene) nanocomposites in ambient conditions is proposed. The nanocomposites were found to be efficient electrocatalysts for ethanol oxidation reaction in alkaline medium. Based on the results of our study, we conclude that Au-PANI nanocomposite is the best electrocatalyst material among all the nanocomposites studied in this work due to its low activation energy and higher electro-oxidation current. The other Au-CP nanocomposites although show a low onset potential value for ethanol electro-oxidation, still require relatively higher activation energies. We believe that the studies reported here for the Au and conducting polymer nanocomposites as anode material for ethanol electro-oxidation will have useful implications in the development of more efficient electrocatalyst for direct alcohol fuel cells.

Acknowledgement

We would like to thank Mr. A. Dhason for his help in AFM imaging. Mr. V. K. William Grips, National Aerospace Laboratory (NAL) for help in SEM studies.

Appendix A. Supplementary data

Supplementary data associated with this article can be found, in the online version, at http://dx.doi.org/10.1016/j.apcatb.2012.06.002.

References

[1] E. Antolini, Applied Catalysis B: Environmental 100 (2010) 413.
[2] V. Selvaraj, M. Alagar, I. Hamerton, Applied Catalysis B: Environmental 73 (2007) 172.
[3] S. Holdcroft, B.L. Funt, Synthetic Metals 28 (1989) C121.
[4] M.F.G. Lyons, D.E. McCormack, P.N. Bartlett, Journal of Electroanalytical Chemistry 261 (1989) 51.
[5] T.N.S. Kumar, A.Q. Contractor, Bulletin of Electrochemistry 6 (1990) 333.
[6] C.T. Hable, M.S. Wrighton, Langmuir 7 (1991) 1305.
[7] C.S.C. Bose, K. Rajeshwar, Journal of Electroanalytical Chemistry 333 (1992) 235.
[8] H. Laborde, J.M. Leger, C. Lamy, Journal of Applied Electrochemistry 24 (1994) 219.
[9] Z. Peng, L. Guo, Z. Zhang, B. Tesche, T. Wilke, D. Ogermann, S. Hu, K. Kleinermanns, Langmuir 22 (2006) 10915.
[10] J. Wang, K.G. Neoh, E.T. Kang, K.L. Tan, Journal of Materials Chemistry 10 (2000) 1933.
[11] (a) P. Rodriguez, Y. Kwon, M.T.M. Koper, Nature Chemistry 4 (2012) 177; (b) B.N. Zope, D.D. Hibbitts, M. Neurock, R.J. Davis, Science 330 (2010) 74.
[12] (a) R.K. Pandey, V. Lakshminarayanan, Journal of Physical Chemistry C 113 (2009) 21596; (b) R.K. Pandey, V. Lakshminarayanan, Journal of Physical Chemistry C 114 (2010) 8507.
[13] M.T. Reetz, W. Helbig, Journal of the American Chemical Society 116 (1994) 7401.
[14] M.T. Reetz, W. Helbig, S.A. Quaiser, U. Stimming, N. Breuer, R. Vogel, Science 267 (1995) 367.
[15] G. Li, C. Maritinez, S. Semancik, Journal of the American Chemical Society 127 (2005) 4903.
[16] S. Kirchmeyer, K. Reuter, J.C. Simpson, in: T.A. Skotheim, J.R. Reynolds (Eds.), Conjugated Polymers – Theory Synthesis Properties and Characterization, 3rd edition, CRC Press Taylor & Francis Group, Boca Raton, FL, 2007.
[17] D.W. Hatchett, M. Josowicz, J. Janata, Journal of Physical Chemistry B 103 (1999) 10992.
[18] D.W. Hatchett, M. Josowicz, J. Janata, Journal of the Electrochemical Society 146 (1999) 4535.
[19] Y.W. Wei, K.F. Hsueh, G.-W. Jang, Macromolecules 27 (1994) 518.
[20] S. Quillard, G. Louarn, S. Lefrant, A.G. MacDiarmid, Physical Review B 50 (1994) 12496.
[21] X.-R. Zeng, T.-M. Do, Journal of Polymer Physics 35 (1997) 1993.
[22] F. Mohammad, Journal of Physics D: Applied Physics 31 (1998) 951.
[23] S.V. Vasilyeva, M.A. Vorotyntsev, I. Bezverkhyy, E. Lesniewska, O. Heintz, R. Chassagnon, Journal of Physical Chemistry C 112 (2008) 19878.
[24] S. Richard, P. Gnanakan, M. Rajasekhar, A. Subramania, International Journal of Electrochemical Science 4 (2009) 1289.
[25] L.M.H. Groenewoud, G.H.M. Engbers, J.G.A. Terlingen, H. Wormeester, J. Feijen, Langmuir 16 (2000) 6278.
[26] S.V. Selvaganesh, J. Mathiyarasu, K.L.N. Phani, V. Yegnaraman, Nanoscale Research Letters 2 (2007) 546.
[27] S. Trasatti, O.A. Petrii, Pure and Applied Chemistry 63 (1991) 711.
[28] N. Hoshi, K. Kida, M. Nakamura, M. Nakada, K. Osada, Journal of Physical Chemistry B 110 (2006) 12480.
[29] Z. Yin, H. Zheng, D. Ma, X. Bao, Journal of Physical Chemistry C 113 (2009) 1001.
[30] F. Ksar, G. Surendran, L. Ramos, B. Keita, L. Nadjo, E. Prouzet, P. Beaunier, A. Hagege, F. Audonnet, H. Remita, Chemistry of Materials 21 (2009) 1612.
[31] R.B. de Lima, H. Varela, Gold Bulletin 41 (2008) 15.
[32] D.H. Nagaraju, V. Lakshminarayanan, Journal of Physical Chemistry C 113 (2009) 14922.
[33] C. Bianchini, P.K. Shen, Chemical Reviews 109 (2009) 4183.
[34] M. Beltowska-Brzezinska, J. Heitbaum, Journal of Electroanalytical Chemistry 183 (1985) 167.
[35] R. Parsons, T. VanderNoot, Journal of Electroanalytical Chemistry 257 (1988) 9.
[36] Z. Borkowska, A. Tyomsiak-Zielinska, R. Nowakowski, Electrochimica Acta 49 (2004) 2613.
[37] H. Angerstein-Kozlowska, B.E. Conway, B. Barnett, J. Mozota, Journal of Electroanalytical Chemistry 100 (1979) 417.
[38] H. Angerstein-Kozlowska, B.E. Conway, A. Hamelin, Journal of Electroanalytical Chemistry 277 (1990) 233.
[39] A. Chen, J. Lipkowski, Journal of Physical Chemistry B 103 (1999) 682.
[40] S.-G. Sun, A. Chen, Electrochimica Acta 39 (1994) 969.
[41] D. Chu, S. Gilman, Journal of the Electrochemical Society 143 (1996) 1685.
[42] Y. Su, C. Xu, J. Liu, Z. Liu, Journal of Power Sources 194 (2009) 295.
[43] C. Jia, H. Yin, H. Ma, R. Wang, X. Ge, A. Zhou, X. Xu, Y. Ding, Journal of Physical Chemistry C 113 (2009) 16138.
[44] A. Aramata, M. Masuda, Journal of the Electrochemical Society 138 (1991) 1949.
[45] S.L. Gojkovic, T.R. Vidakovic, D.R. Durovic, Electrochimica Acta 48 (2003) 3607.